NASA CR-144001

FINAL REPORT

Discrete Component Bonding and Thick Film Materials Study

Contract No. NAS8-30883

Period Covered: July 1, 1974 - August 31, 1975

Prepared for

George C. Marshall Space Flight Center
Marshall Space Flight Center, Alabama 35812

Prepared by

D. L. Kinser
Vanderbilt University
Department of Materials Science and Engineering
Nashville, Tennessee 37235

(NASA-CR-144001) DISCRETE COMPONENT BONDING AND THICK FILM MATERIALS STUDY Final Report, 1 Jul. 1974 - 31 Aug. 1975 (Vanderbilt Univ.) 38 p HC $3.75 CSCL 11A

N76-10318

Unclas
G3/27 39427

Reported:

September 17, 1975

Abstract: This report summarizes the results of an investigation of discrete component bonding reliability and a fundamental study of new thick film resistor materials. The component bonding study examined several types of solder bonded components with some processing variable studies to determine their influence upon bonding reliability. The bonding reliability was assessed using the thermal cycle: 15 minutes at room temperature, 15 minutes at +125°C 15 minutes at room temperature and 15 minutes at -55°C. One of the process variables examined was ultrasonic stress relief of the soldered system before subjecting it to the thermal cycling. The thick film resistor materials examined were of the transition metal oxide-phosphate glass family with several elemental metal additions of the same transition metal. These studies were conducted by preparing a paste of the subject composition, printing, drying and firing using both air and reducing atmospheres. The resulting resistors were examined for adherence, resistance, thermal coefficient of resistance and voltage coefficient of resistance. One of the iron oxide-phosphate glass compositions appears to be a promising candidate for commercial applications.

TABLE OF CONTENTS

LIST OF TABLES

LIST OF FIGURES

THERMAL CYCLING STUDIES

Objective

The objective of this portion of our program was to distinguish the processing variables which influence reliability in thermal cycling. The processing variables examined included solder composition, pretinning, quenching rate from soldering temperature, and ultrasonic stress relief after soldering.

Experimental Technique

For purposes of experimental evaluation of processing variables the substrate chosen was American Lava Type 614 with commercial surface finish. The conductor metallization chosen was Dupont Type 8553, a high reliability platinum-gold thick film metallization. The solders chosen were Kesters eutectic type with 63 tin and 37 lead and the 96 tin 4 silver. The flux employed was also Kester type 1544A. The capacitor chips employed in this study were the Union Carbide Chemet type 10^4 picofarad ≠20% 50 volt rated with BX type dielectric. The capacitor terminations were pretinned with solder of the above mentioned types. The physical dimensions of these capacitors were 0.444 x 0.318 x 0.152 cm (0.175 x 0.125 x 0.060 inch).

The capacitors were mounted on a standard metallization pattern with 25 chips on each substrate. The metallization was printed, dried and fired in accord with the manufacturers instructions. The substrates were pretinned after fluxing by dipping for 5 seconds at 300°C for 63/37 solder and 250°C for 96/4 solder. The substrates were removed from the tinning bath in a vertical

position to facilitate drainage of excess solder. The capacitors were placed in their positions and the substrate was placed on a hotplate at 300°C for 63/37 solder and 250°C for 96/4 solder where it was held until the solder reflowed or for approximately 5 seconds and then cooled as shown in Figure 1. The two basic cooling rates were obtained by placing the substrate on a room temperature aluminum block and by cooling on the hotplate with insulation to slow cooling.

After the soldering operation the flux was removed from the substrates with toluene and the solder joints were visually inspected. One group of bonded capacitors was subsequently subjected to ultrasonic stress relief treatment. This operation was conducted in a conventional cleaning type ultrasonic unit by immersing the substrate in benzene and operating the unit for 120 minutes. After the substrates had been prepared as described above, they were thermally cycled using a specially designed apparatus. This apparatus consisted of an insulated chamber held at +125°C ± 2°C, a second chamber cooled by dry ice at -55°C and a mechanical arm to transfer the samples from ambient to each chamber. This allowed the standard cycle 15 minutes at ambient, 15 minutes at +125°C, 15 minutes at ambient and 15 minutes at -55°C to be repeated for up to 1000 cycles. The initial setup employed an electrical monitor of each substrate which detected the electrical failure of a single chip on any of the 10 substrates in the test apparatus. This monitor was changed to a manual monitor in the course of the cycling because of electrical connection problems

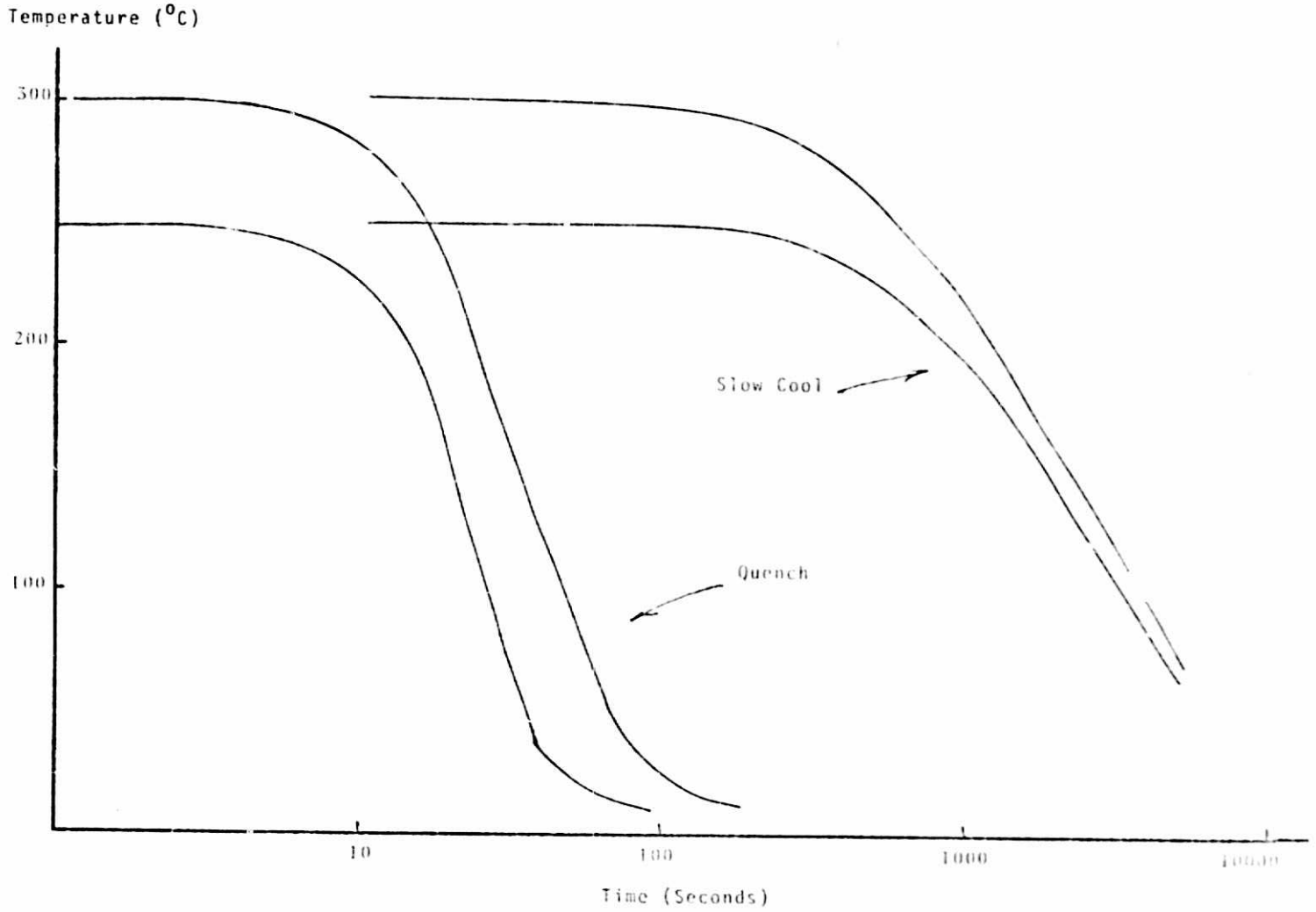

Figure 1. Cooling curves for the soldering process. Quenching corresponds to removing the substrate from heat source and placing on cold aluminum block while the slow cool corresponds to cooling the sample on a hot-plate with insulation.

to the substrate caused by alternate icing and melting. The final results are thus the collective data from electrical monitoring and visual inspections conducted after each 10 to 40 cyles.

Results

The results of these experiments are presented in the form of cumulative percentage of failures as a function of number of thermal cycles. The results of cycling on the 63 Sn-37 Pb soldered system without pretinning of the substrate metallization are shown in Figure 2. The data here are quite scanty because the high failure rate at 100 cycles caused us to terminate the cycling at 300 cyles where the failure rate reached 18%. It is quite apparent that the reliability of capacitors bonded with this technique is most unsatisfactory for use in high reliability systems.

The results of the customary soldering operation with 63 Sn-37 Pb solder with a rapid quench from the soldering temperature are shown in Figure 3. The failure rate in this system reaches 20% at 600 cycles and is thus considerably better than the untinned technique but the system is certainly unacceptable at this high number of cycles. It should be noted that reproducibility of this soldering technique was quite variable. Two substrates with a total of 100 bonds (50 chips) were cycled and one of the substrates with 50 bonds survived the 1000 cycles with no failures. The data, however, are based upon two substrates and the poorer substrate suffered a 40% failure rate at 600 cycles hence the soldering technique is of questionable reproducibility.

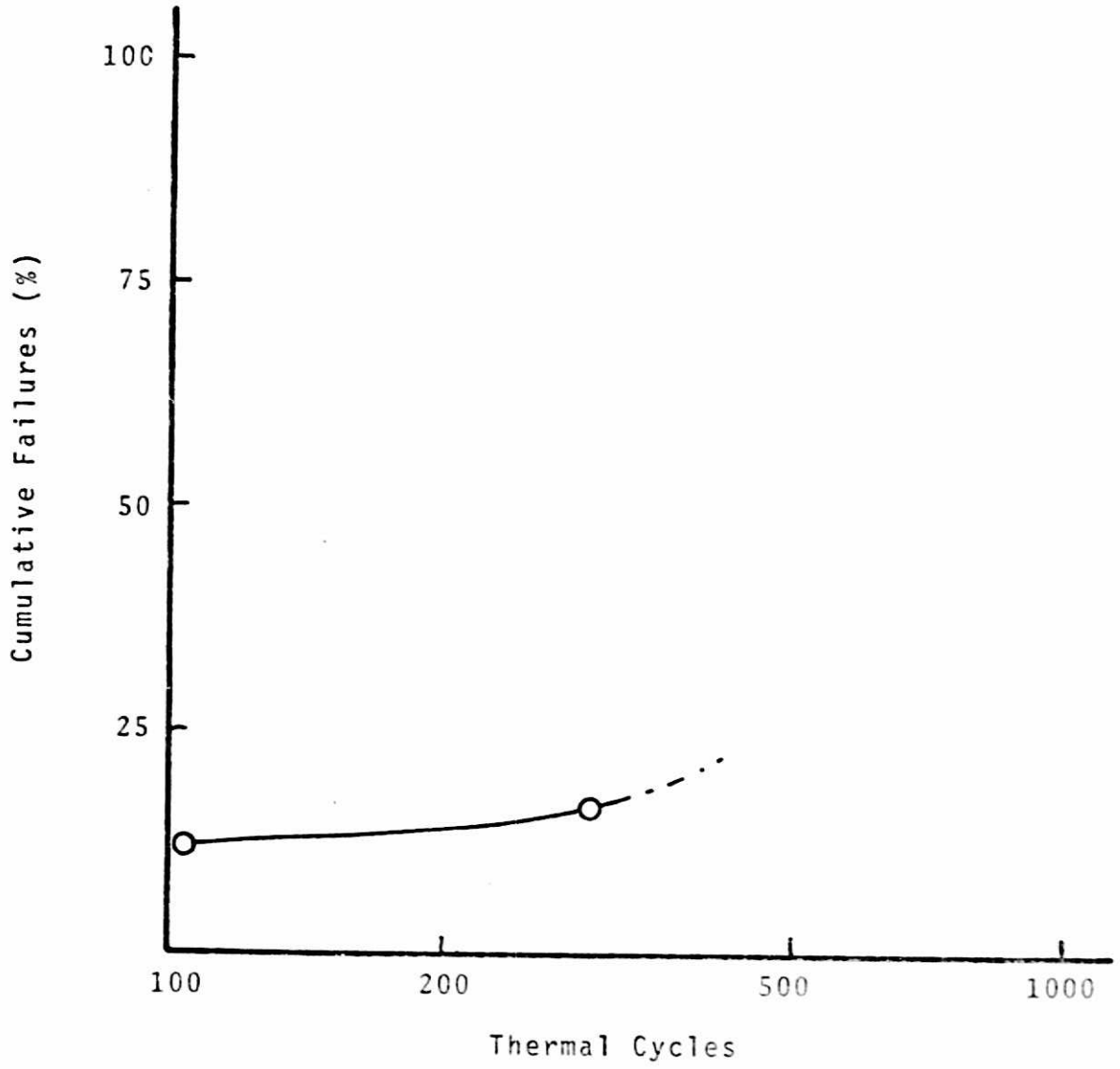

Figure 2. Cumulative failures as a function of number of thermal cycles for samples of 63 Sn-37 Pb without a pretinning treatment.

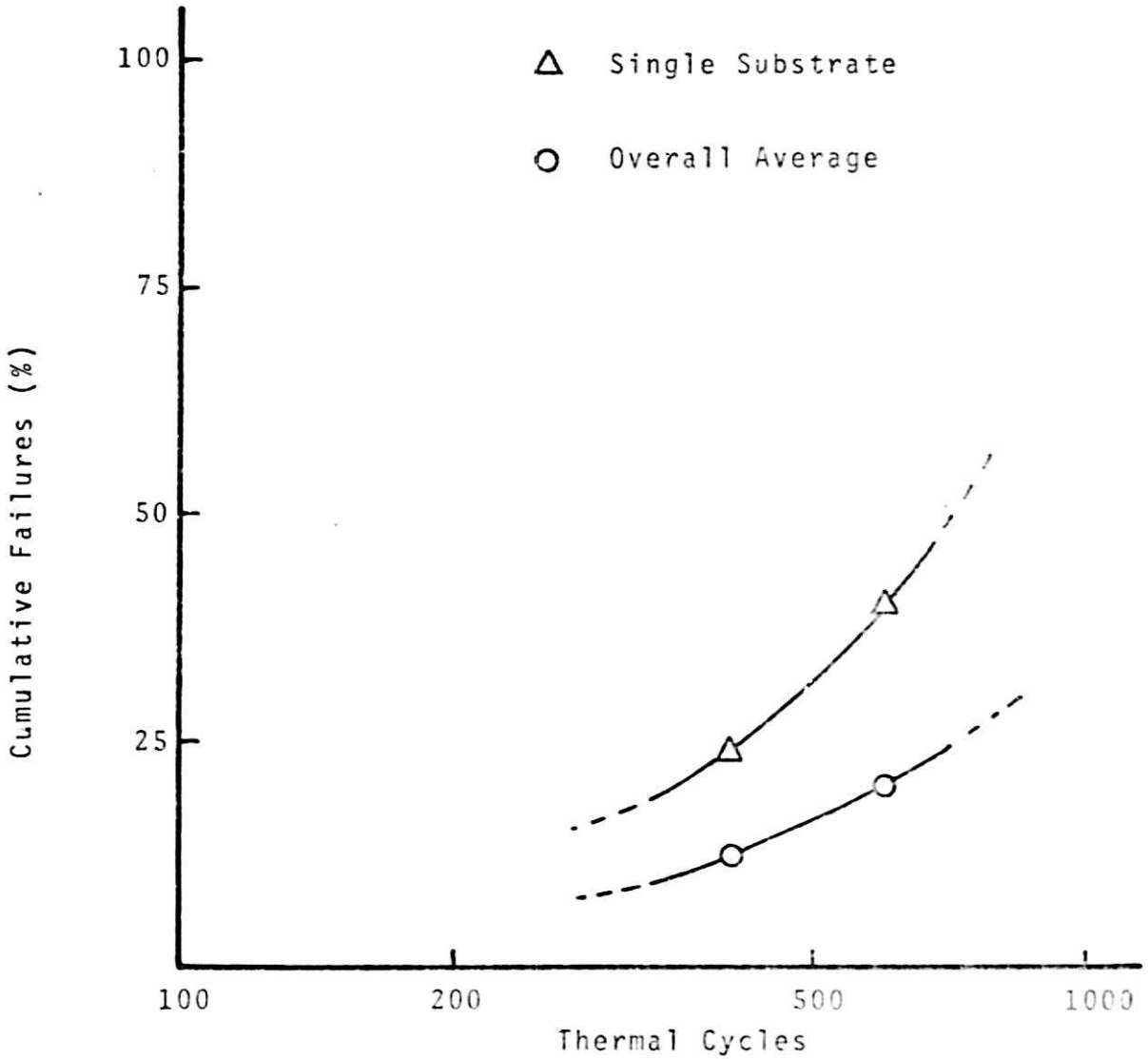

Figure 3. Cumulative failures as a function of number of thermal cycles for samples of 63 Sn-37 Pb quenched from the soldering temperature.

There are no known differences in the processing techniques for these substrates hence it appears that the technique produces bonds of rather widely variable behavior. The results obtained on a 63 Sn-37 Pb solder slowly cooled from the soldering temperature are shown in Figure 4. It is apparent that the variation from substrate to substrate is quite large and large failure rates are noted. One of the substrates had 24 of the 25 capacitors with electrical failure (96% failure rate) at 1000 cycles. The second substrate had only 16% failures at 700 cycles. Again no processing variables were known to have changed during the process hence no explanation for the variability can be advanced. This substrate also exhibited a second failure mechanism not previously noted. The pretinned metallization lines on these substrates are severely degraded during thermal cycling and some electrical failures occured in the metallization. This type behavior is apparent in the photograph shown in Figure 5.

The results of cycling upon an ultrasonically stress relieved 63 Sn-37 Pb are shown in Figure 6. It is immediately clear that the stress relief treatment has not enhanced the performance of this solder bond under thermal cycling. The best of the two substrates subjected to this treatment exhibited a 77% failure rate at 1000 cycles while the worst failure rate reached 96% at 900 cycles. The stress relief treatment has clearly degraded the performance of this solder and the untreated system (Figures 3 and 4) has clearly superior reliability.

The 96 Sn-4 Ag solder with a slow cool from soldering temperature was subjected to thermal cycling and the results of

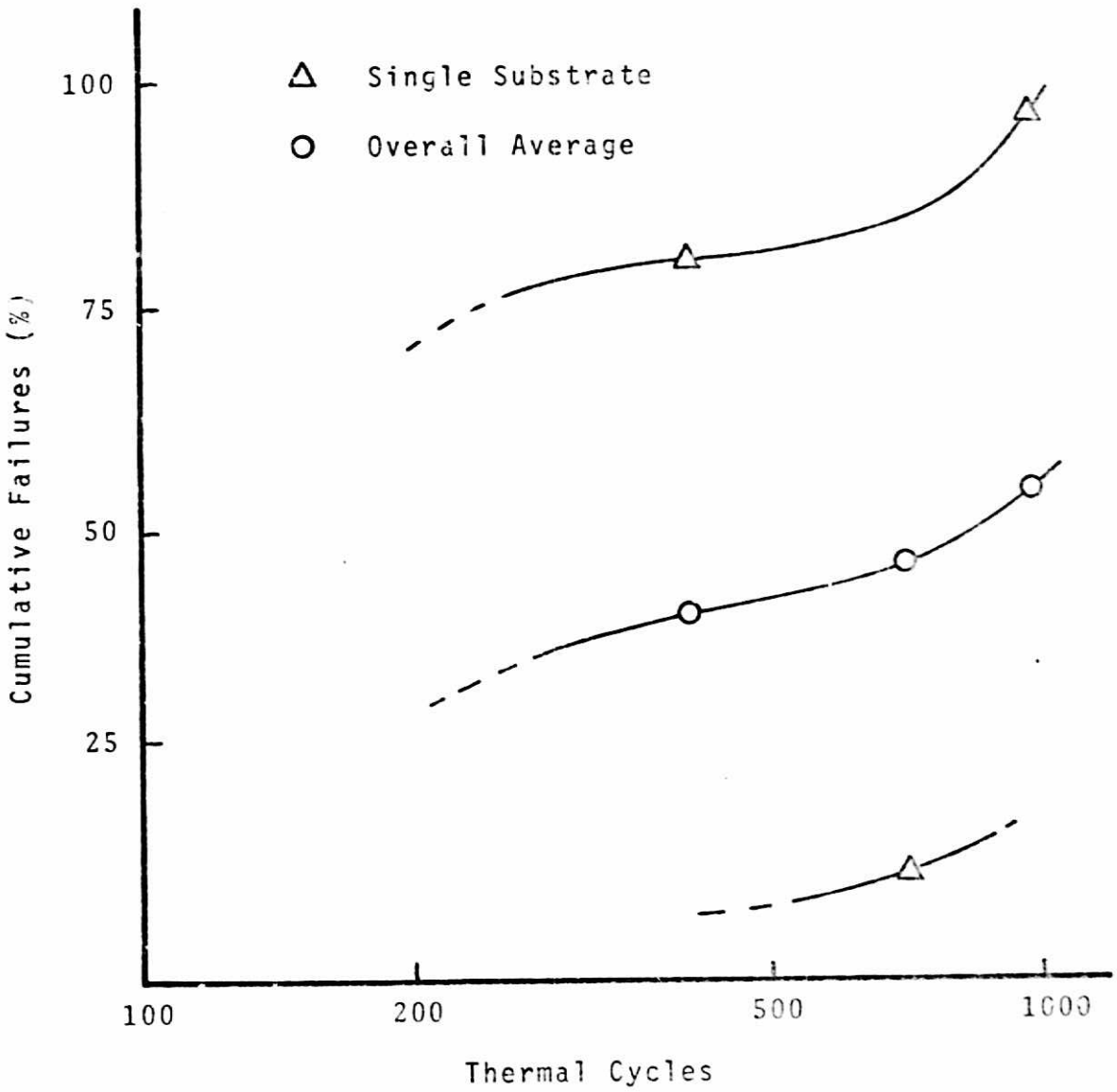

Figure 4. Cumulative failures as a function of number of thermal cycles for samples of 63 Sn-37 Pb slow cooled from the soldering temperature.

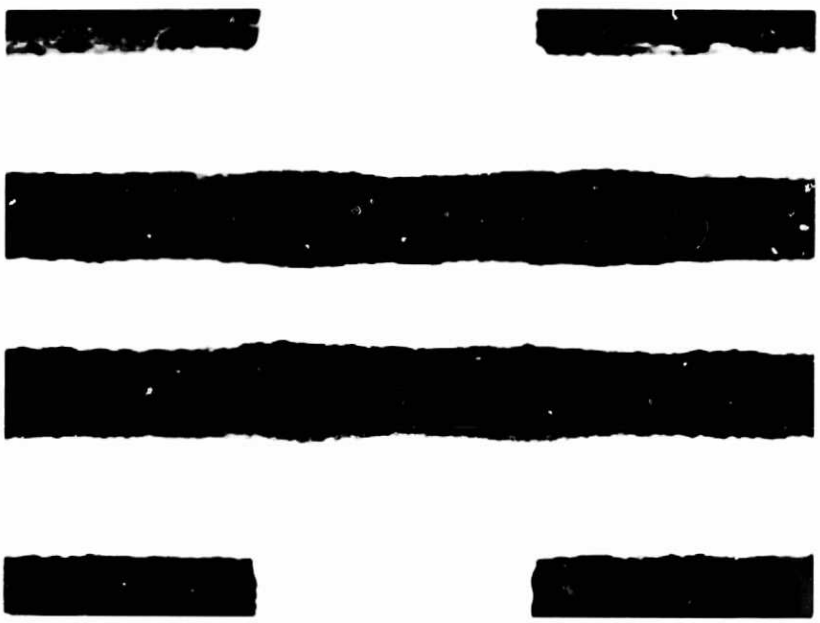

Figure 5. Typical metallization failure during thermal cycling. Illumination is from back of substrate to highlight the crack thus metallization appears black.

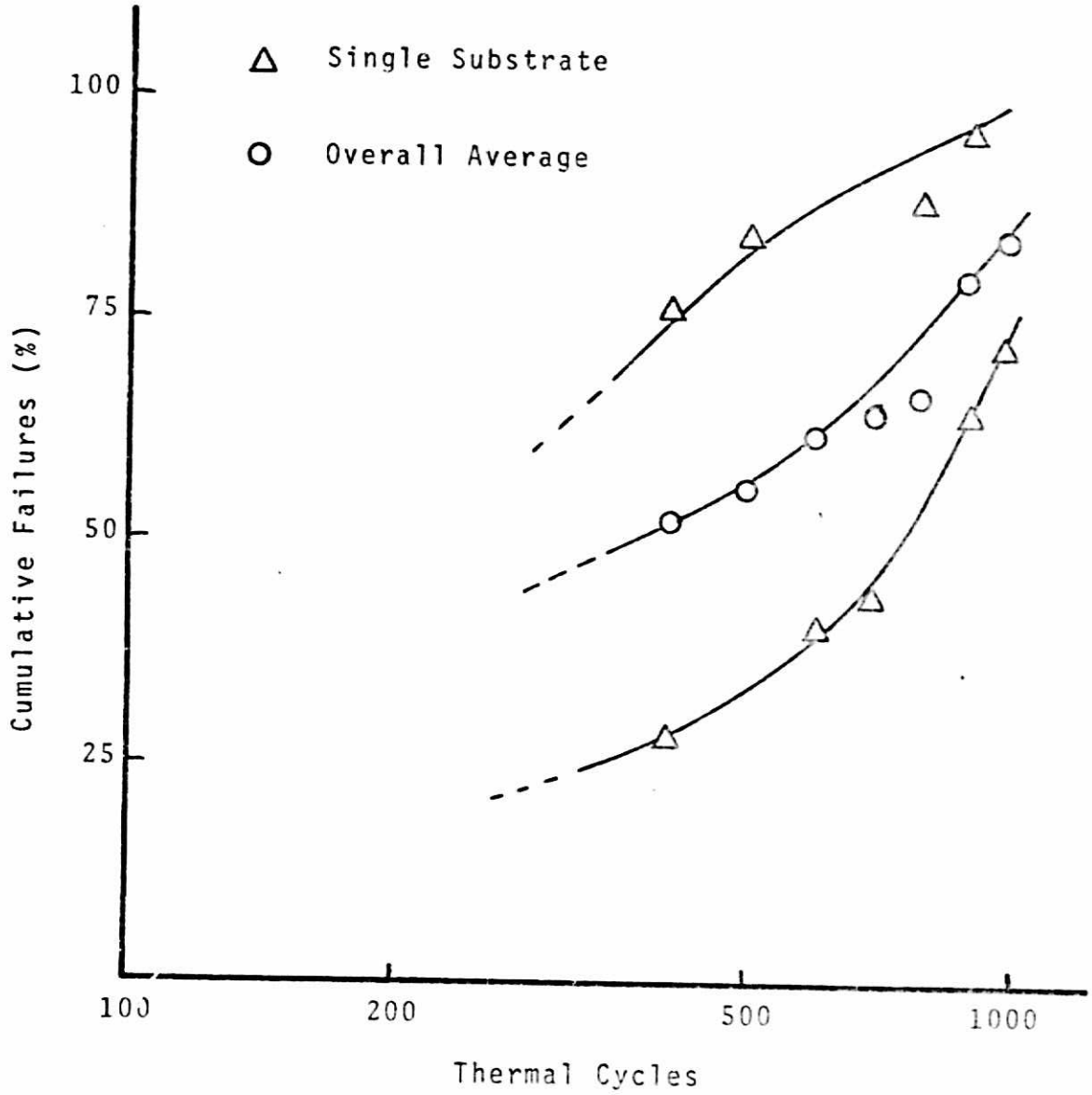

Figure 6. Cumulative failures as a function of number of thermal cycles for samples of 63 Sn-37 Pb slow cooled from the soldering and ultrasonically stress relieved before thermal cycling.

this are shown in Figure 7. The variability from sample to sample in this system is considerably lower than in the 63 Sn-37 Pb solders but the overall reliability is unquestionably lower. This system exhibits failure rates as high as 38% at 265 cycles and is thus poorer than the tin/lead solder. The results of a 96 Sn-4Ag solder quenched from soldering temperature to ambient are shown in Figure 8. It is apparent that the variability from sample to sample in this system is quite small in comparison with all other samples examined. Unfortunately, the reliability of this solder is so low that 100% failure was reached at 850 cycles. Each class of capacitor solder bond was examined in a destructive manner by standard metallographic techniques. The capacitor-bond-substrate was sectioned along the longitudinal axis of the capacitor perpendicular to the substrate using a diamond saw and the resulting section was metallographically polished using diamond abrasives. These sections were examined in the microscope in order to determine the origin of the macroscopically observed cracks in the solder. A typical example of these sections is shown in Figure 9 which is a 63/37 solder which was quenched from the soldering temperature. It is clear that the crack initiated near the surface and propagated in a manner which virtually removed a portion of the near surface solder. This crack appears to have branched and started under the capacitor at near its midpoint although this crack has not released the capacitor from the substrate.

A separate observation made in the course of this study was the severe degradation of the metallization which had been

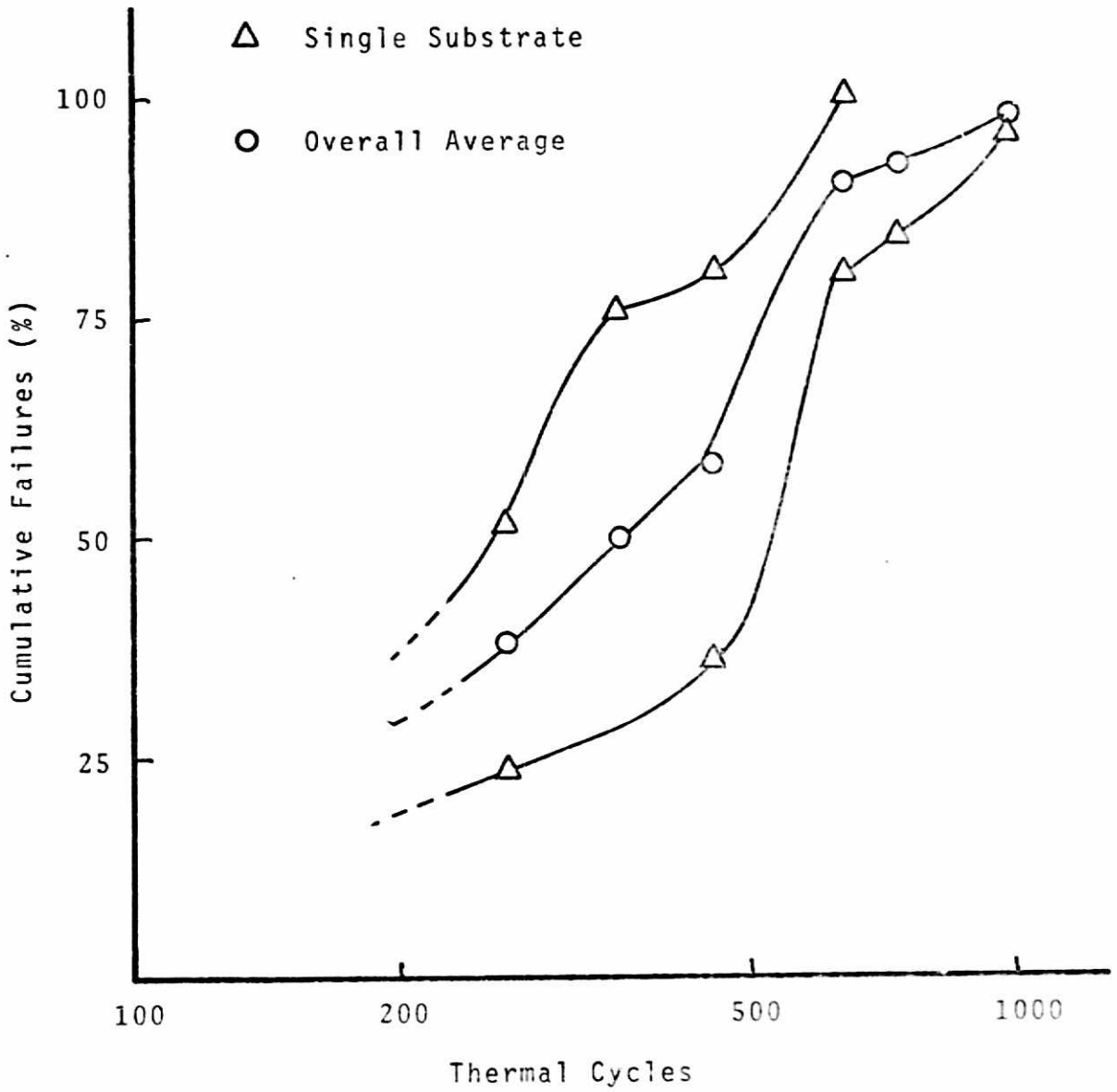

Figure 7. Cumulative failures as a function of number of thermal cycles for samples of 96 Sn-4 Ag solder slow cooled from the soldering temperature.

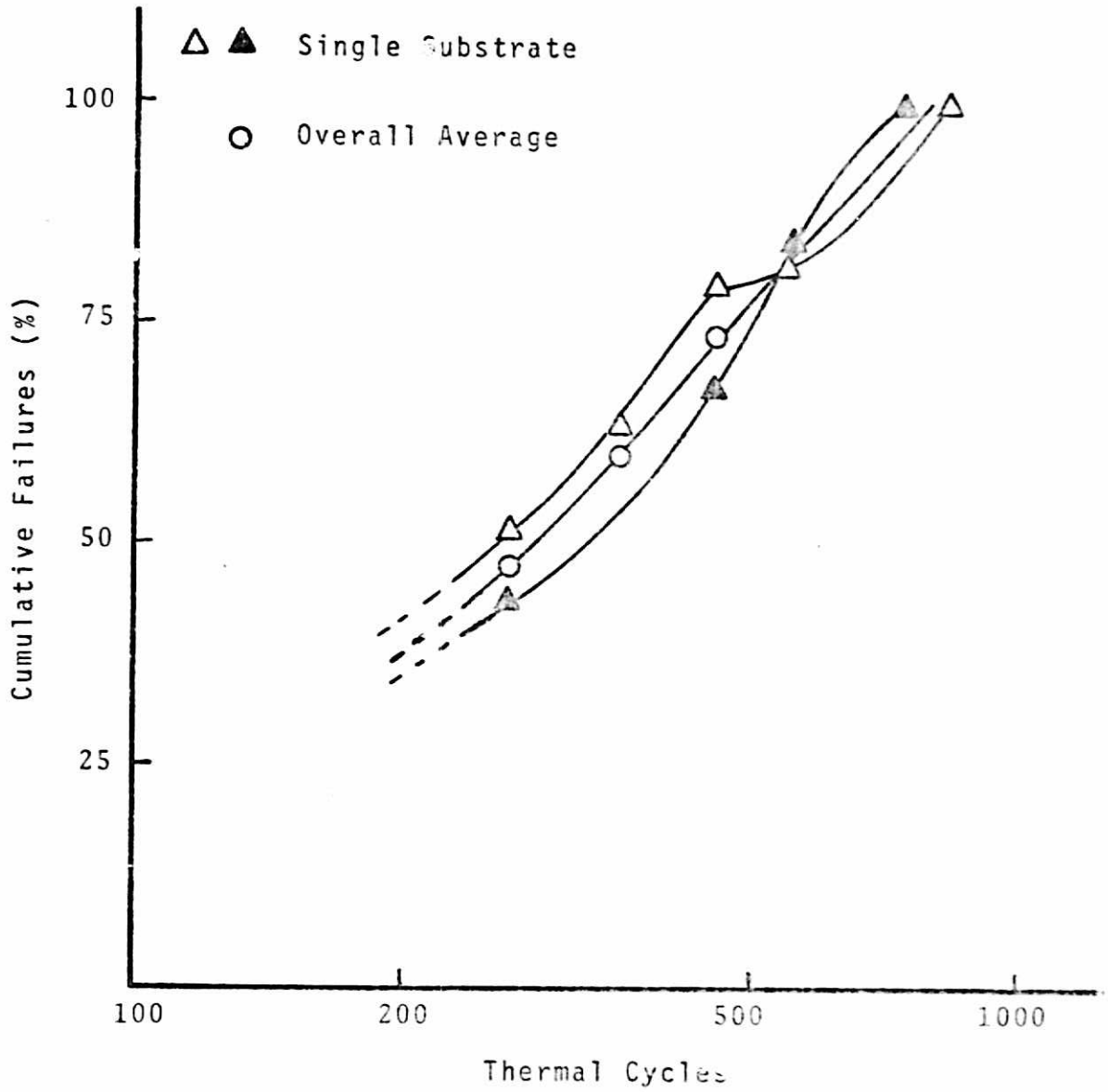

Figure 8. Cumulative failures as a function of number of thermal cycles for samples of 96 Sn-Ag quenched from the soldering temperature.

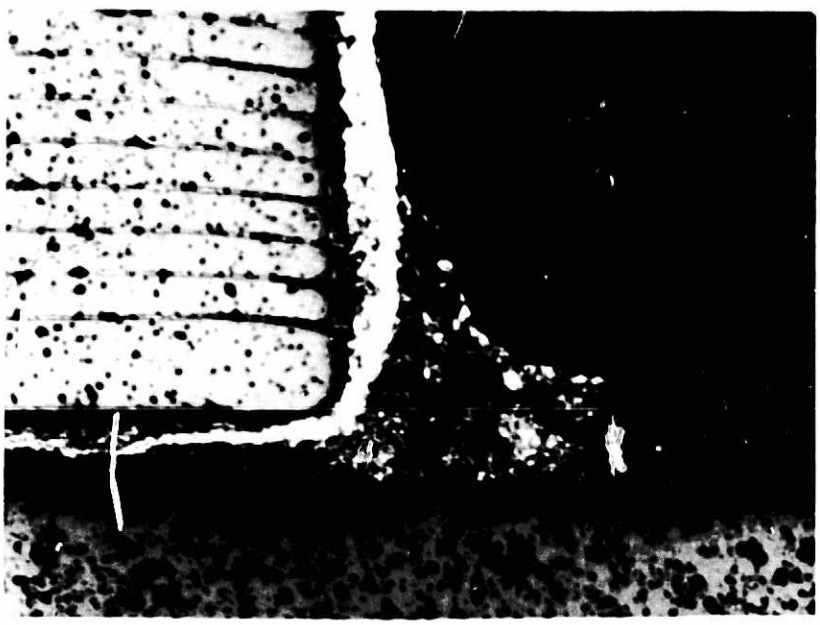

Figure 9. Cross section of capacitor chip/solder/metallization/substrate for a typical capacitor bond after thermal cycling. Some samples appeared to have lost pieces such as the one shown here in the intact position with almost complete crack.

pretinned. Many of the conductors were severely eroded from points near corners and other stress concentrators and some of the conductors had actual cracks which resulted in electrical opens. Figure 5 is an example of the more severe state of this phenomena and shows the complete breakage of the metallization utilizing backlighting of the substrate.

Discussion of Results

The results of soldering process variables upon the failure behavior during thermal cycling are summarized in Figure 10. It is apparent that the most reliable system examined is the 63 Sn-37 Pb solder quenched from the soldering temperature. The next most reliable bonding system is the untinned 63 Sn-37 Pb quenched from the soldering temperature. The remaining soldering systems are clearly distinguished from one another but the reliability of all these systems leaves much to be desired. It is to be noted that much of the theoretical predictions from previous work in this program are not borne out by the present experimental data. It was, for example, predicted that the more refractory solders would be less degraded by thermal cycling. The 63 Sn-37 Pb solder melts at 183°C while the 96 Sn-4 Ag solder melts at 221°C but the less refractory solder is the more reliable of the two. We are unable to advance a reason for this disagreement with our theoretical predictions. The metallurgical analysis of the effect of cooling rates upon the residual stresses in thermally cycled systems indicated that a slower cooling rate should leave less stress in the capacitor and thus produce a lower failure rate. Comparison of the data in Figure 10 for quenched

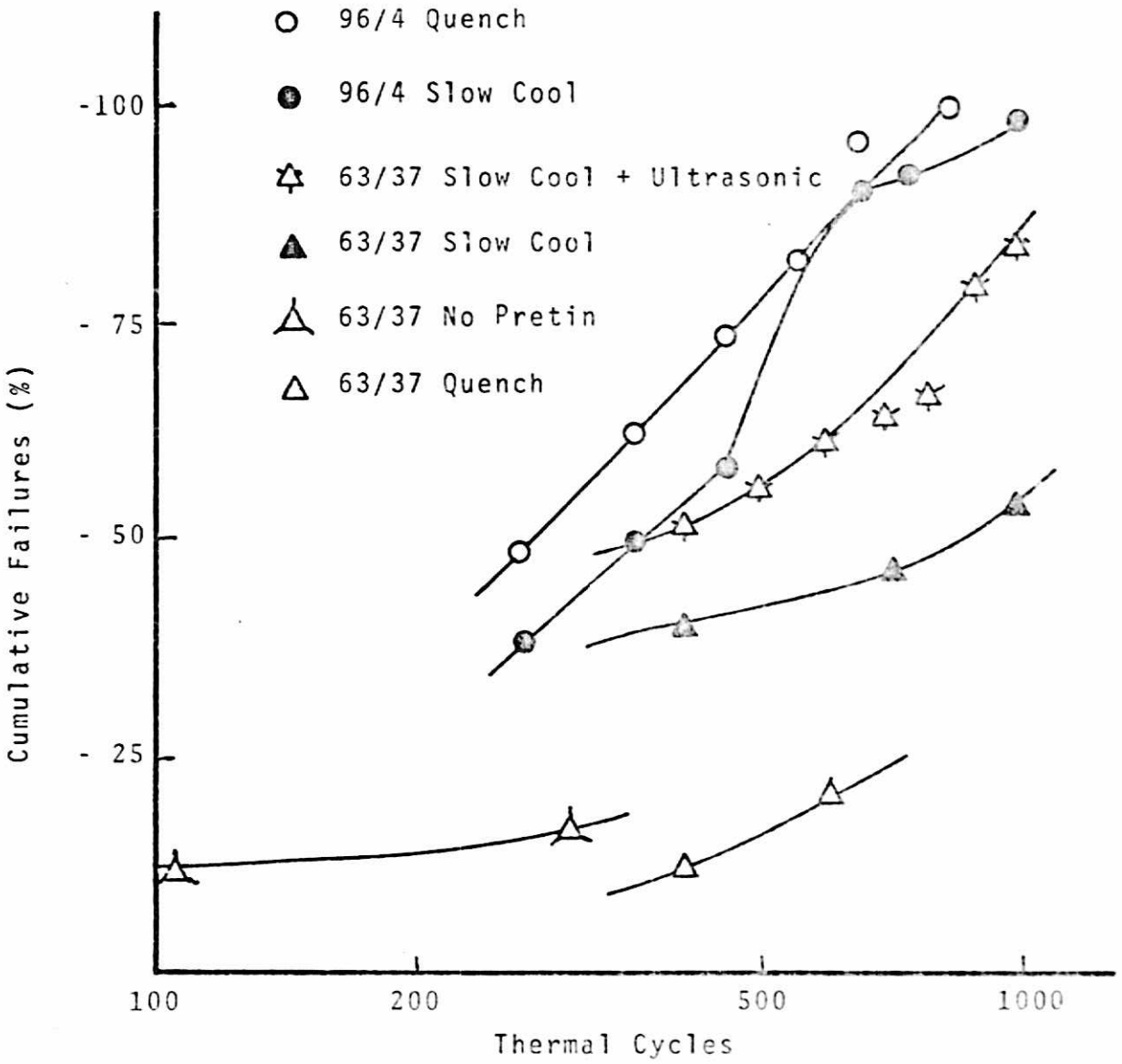

Figure 10. Summary of the overall cumulative failure behavior as a function of number of thermal cycles.

and slow cooled 63 Sn-37 Pb solder indicates that the quenched sample is clearly more reliable thus again contradicting our theoretical predictions. The effect of cooling rate in the 96 Sn-4 Ag solder is, as predicted, to lower the failure rate for lower cooling rates. This solder which behaves as predicted from theoretical analyses unfortunately exhibits such high failure rates even after slow cooling as to render it unusable as a bonding system.

The analysis of ultrasonic stress relief treatments upon the residual stress in the capacitor chip indicated that an ultrasonic stress relief treatment should increase the reliability of the system. The observed effect of this treatment is to render this particular system and treatment the least reliable of the family of 63 Sn-37 Pb solder treatments examined. This may possibly be the result of too long a 'stress relief' resulting in the initiation of cracks by mechanical fatigue in the solder but detailed scanning electron microscopy will be necessary to confirm this failure mode.

In the course of this study we have also noted a previously unreported failure mode in the substrate metallization. This failure mode takes the form of a reaction between the solder and the platinum/gold metallization and leads to loss of electrical continuity in the conductor. This may be the consequence of two possible failure modes. The most likely mode appears to be the differential thermal expansion between substrate, substrate metallization and solder. None of these components can be expected to

have the same thermal expansion coefficient hence mechanical stresses are created during thermal cycling. This could lead to the observed cracking and is supported by the preponderance of cracks initiating at corners and other locations of stress concentration. The second possible metallization/solder failure mode is the formation of an intermetallic compound or compounds by interdiffusion of the solder and substrate metallization. There are four elements present to form intermetallic compounds hence there are almost innumerable possible intermetallic compounds which can be formed.

Conclusions

1. The effect of solder composition appears to be unpredictable from theoretical analyses based upon first principles. The refractory solder examined in this program is considerably less reliable than the common soft solder.

2. The effect of cooling rate from soldering temperature is not consistent from solder to solder and no generalizations based on experimental or theoretical bases can be made at this time.

3. Previously unreported degradation of thick film metallization by solder indicates serious concern for reliability of systems employing solder with thick film metallization.

4. Solder bonded systems which have been examined in this program are far too unreliable to be seriously considered for use in high reliability space or military systems.

RESISTOR PASTE STUDIES

Introduction

Previous studies of transition metal oxide glasses as thick film resistors[1] indicated that properties of phosphate glasses were similar to bulk glass properties and phosphates were more stable than other glasses. Recent studies of electrical properties of bulk iron phosphate glass[2] recommend it as a candidate for thick film resistor pastes.

Iron phosphate glass of several compositions was ground and combined with an organic vehicle of ethyl-cellulose and alpha terpineol. Rheology was optimized by controlling the composition of the organic vehicle and the ratio of glass frit to organic vehicle in the paste. Firing conditions include controlled time temperature profiles and reducing or oxidizing atmospheres.

The effects of firing cycle and composition were correlated with electrical measurements including resistance voltage and temperature coefficients of resistance.

Theory

Many transition metal oxides form glasses with P_2O_5. Electrical properties of iron phosphate glass have been reported by Vaughan[3] and Dozier.[4] Semiconducting behavior generally occurs when the transition metal exists in more than one valence state allowing conduction to take place by transfer of electrons from low valence to high valence states. Because of the nature of charge transport the ratio of Fe^{2+}/Fe^{total} is important in controlling conductivity.

Thermal history of bulk glass samples has been shown to

affect conductivity with increasing quenching rates in the casting process decreasing density and increasing separation of the iron ions resulting in higher resistivity. Annealing bulk samples alters conductivity by changing the effective Fe^{2+}/Fe^{total} ratio. Growth of crystals during annealing may effectively remove Fe^{2+} or Fe^{3+} ions from the conduction process if either ion is tied up in the crystalline phase.

Experimental Procedure

As initial candidates, iron phosphate glass of three compositions were used in two and three component pastes. The two component pastes consisted of glass powder and an organic vehicle (OV). The addition of iron oxide (Fe_2O_3) or iron metal powder made a three component paste as shown in Table I. Two OV's of 20.0 and 26.8 grams of ethyl cellulose per liter of alpha-terpineol were used to allow optimization of printing characteristics. Particle sizes were controlled by sieving down to 37 microns. Sizes down to 1 micron were ground by ball milling and monitored by the scanning electron microscope. The pastes were dried in air at 80°C for 30 minutes and fired at several peak temperatures in reducing and oxidizing atmospheres.

The oxidizing furnace employed programmable temperature/time capability to give temperature/time profiles as shown in Figure 11. Hydrogen gas was used as the reducing atmosphere in a fixed temperature gradient furnace with the temperature/time profile controlled by substrate position. Figure 12 shows the details of atmosphere control for the furnace. Electrical characteristics were studied by resistance and voltage and temperature

TABLE I. Glass Compositions Studied

	Glass				Total Iron Oxide	Total Iron
	FeO A/o	Fe_2O_3 A/o	P_2O_3 A/o	Added	A/o	A/o
A	23.0	17.0	60.0	--	40.0	--
B	33.2	7.7	59.1	Fe_2O_3	70.0	--
C	42.0	8.33	49.67	Fe	--	70.0

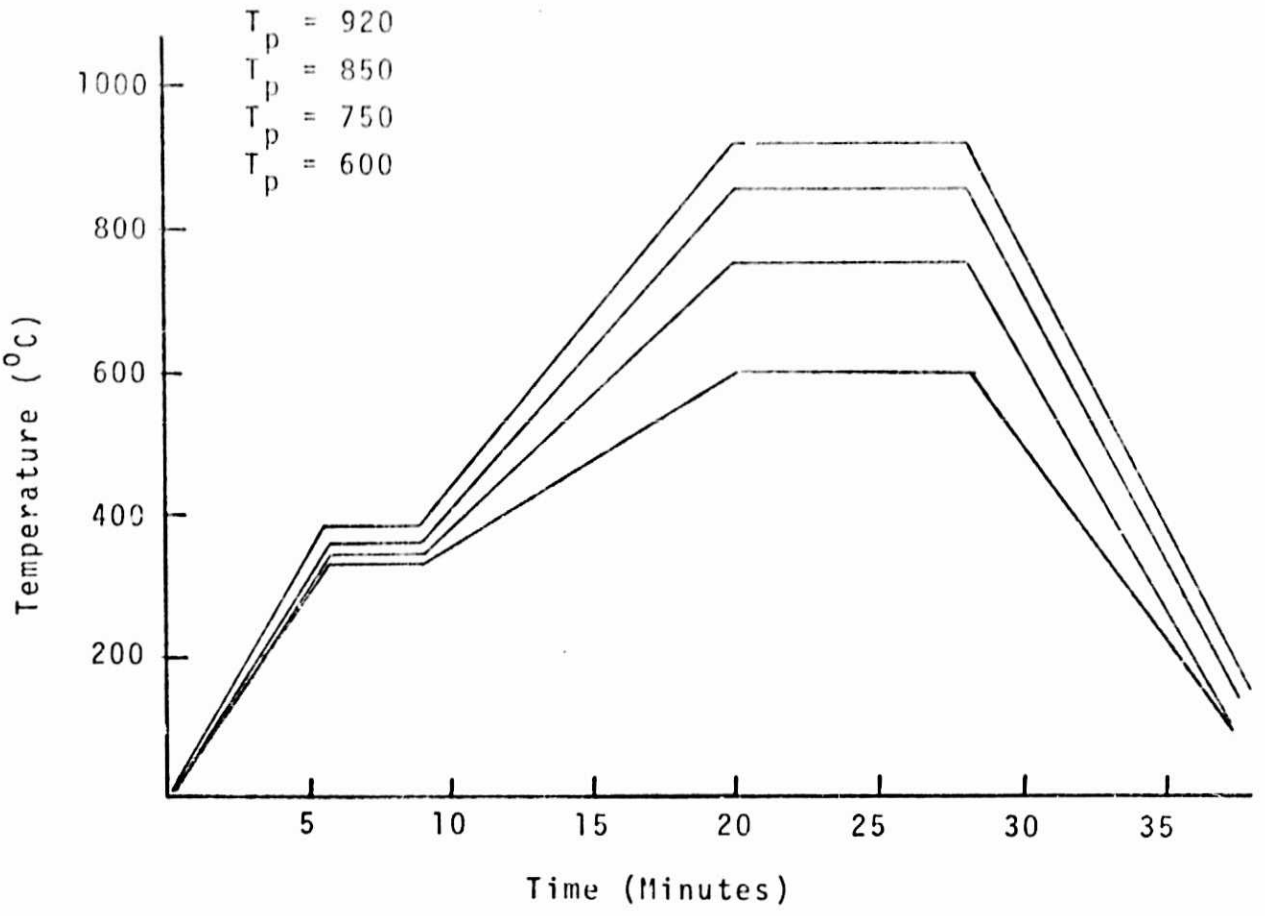

Figure 11. Temperature as a function of time for the programmable furnace (firing profile).

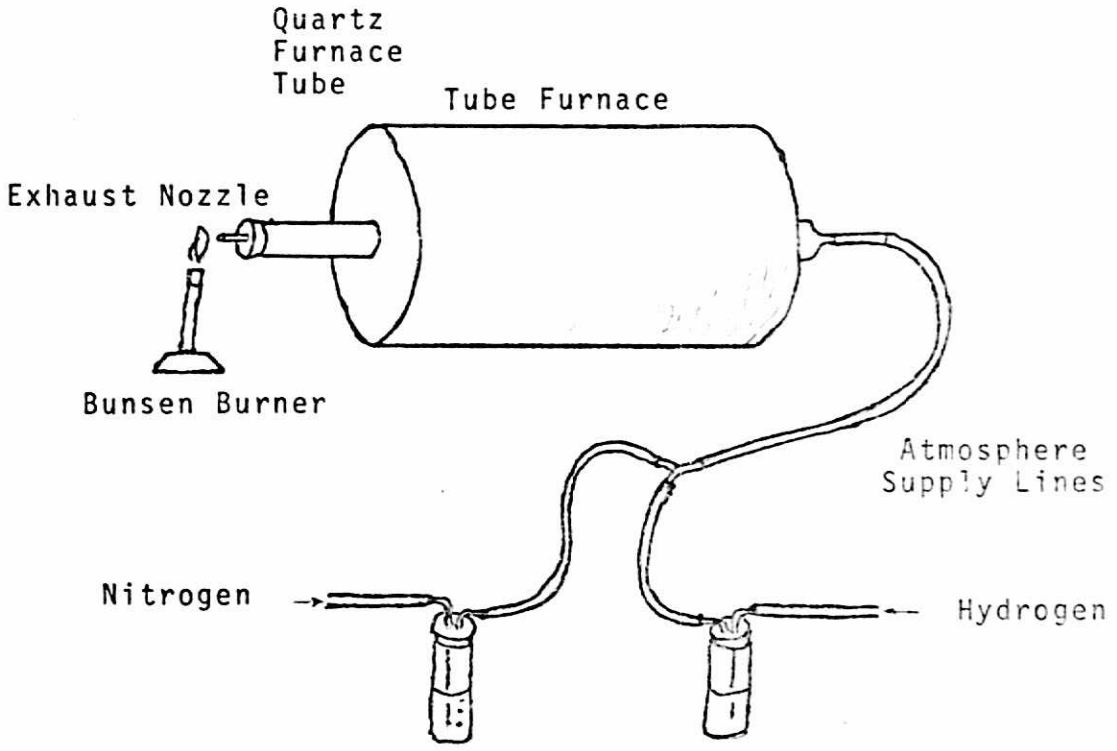

Figure 12. Schematic diagram of the reducing atmosphere furnace.

coefficients of resistance (VCR and TCR).

Discussion of Results

Rheology. Glass particle size, composition and amount of OV, storage time and amount of thinners used affected rheology.

Particle sizes used varied from 1 to 37 microns, limited on the upper bound by screen mesh. As the particle size approached the screen mesh limits the surface of the printed resistor became discontinuous and the amount of paste transferred to the substrate was reduced. Smaller particle sizes increased the general quality of the resistor and ease of printing. Optimum results were attained with an average particle size of 1-3 microns and an upper bound of 7 microns. Samples of the frit were measured with the scanning electron microscope to determine the average particle size. Increasing grinding times made it impractical to prepare particle sizes smaller than 1 micron.

The organic vehicle was ethyl-cellulose dissolved in alpha-terpineol in two compositions; 20.0 and 26.8 grams of ethyl cellulose per liter of alpha terpineol. Greater ease of printability and more uniform resistors were produced from the lower ethyl-cellulose O.V. The 26.8 gms/l paste passed through the screen with greater difficulty and exhibited a tendency to polymerize.

The quality of the resistors was affected by the amount of OV used in the paste. Grainy, hard to print paste resulted if too little O.V. was used and excessive OV resulted in thin resistors and resolution loss if the thin pastes ran. Pastes with 2.5-3.0 grams of glass frit per milliliter of O.V. resulted in optimum printability and visual resistor quality. After three

to four weeks of storage, thinners were often needed to readjust the paste viscosity. Thinners used as needed were diethylene glycol monobutyl ether and diethylene glycol monoethyl ether.

Firing Characteristics.

Firing characteristics of the pastes were studied by varying temperature and atmosphere and are summarized in Tables II and III. Peak firing temperatures ranged from 600°C which is near the softening point of the glass to 950°C. Resistors fired in air had resistances of 10^{11} to 10^{12} ohms/square, however, resistors fired under hydrogen ranged from 5 megaohms/square to 10 ohms/square. The effect of atmosphere change varied with iron content. Change in peak firing temperature from 670°C to 850°C had little effect on paste B changing it only 0.67% but pastes A and C changed from 5 megaohms to 5 kiloohms and 200 ohms to 10 ohms, respectively.

Electrical Characteristics.

Resistance decreased with increasing iron content with 70 A/o iron (C) paste near 10 ohms per square, 70 A/o iron oxide (B) paste near 100 ohms,square and the 40 A/o iron oxide (A) near 5 kiloohms/square. Long term storage data on fired resistors was not available at the time of this report, however, short term indications show need for a stabilization bake or overglaze protection. Surface iron oxidation may be the principal cause of drift indicating an overglaze requirement.

The temperature coefficient of resistance was measured from -60°C to +125°C and percent change versus temperature is plotted in Figure 13. Effect of measurement temperature on

TABLE II.* Relative Adhesion as Related to Firing Condition

Paste	600°C	750°C	850°C	920°C
		Oxidizing Atmosphere		
A	G	P	P	-
B	P	-	P	-
C	P	-	-	G
		Reducing Atmosphere		
A	P	F	G	P
B	P	F	F	P
C	P	P	P	P

* G-Good, F-Fair, P-Poor

TABLE III.* Electrical Resistance as a Function of Firing Temperature in Reducing Atmospheres

Paste	670°C	850°C
A	5 MΩ/□	5 KΩ/□
B	75 Ω/□	80 Ω/□
C	200 Ω/□	10 Ω/□

* All resistors fired in air R $\cong$ 10^{11} - 10^{12} ohms/□.

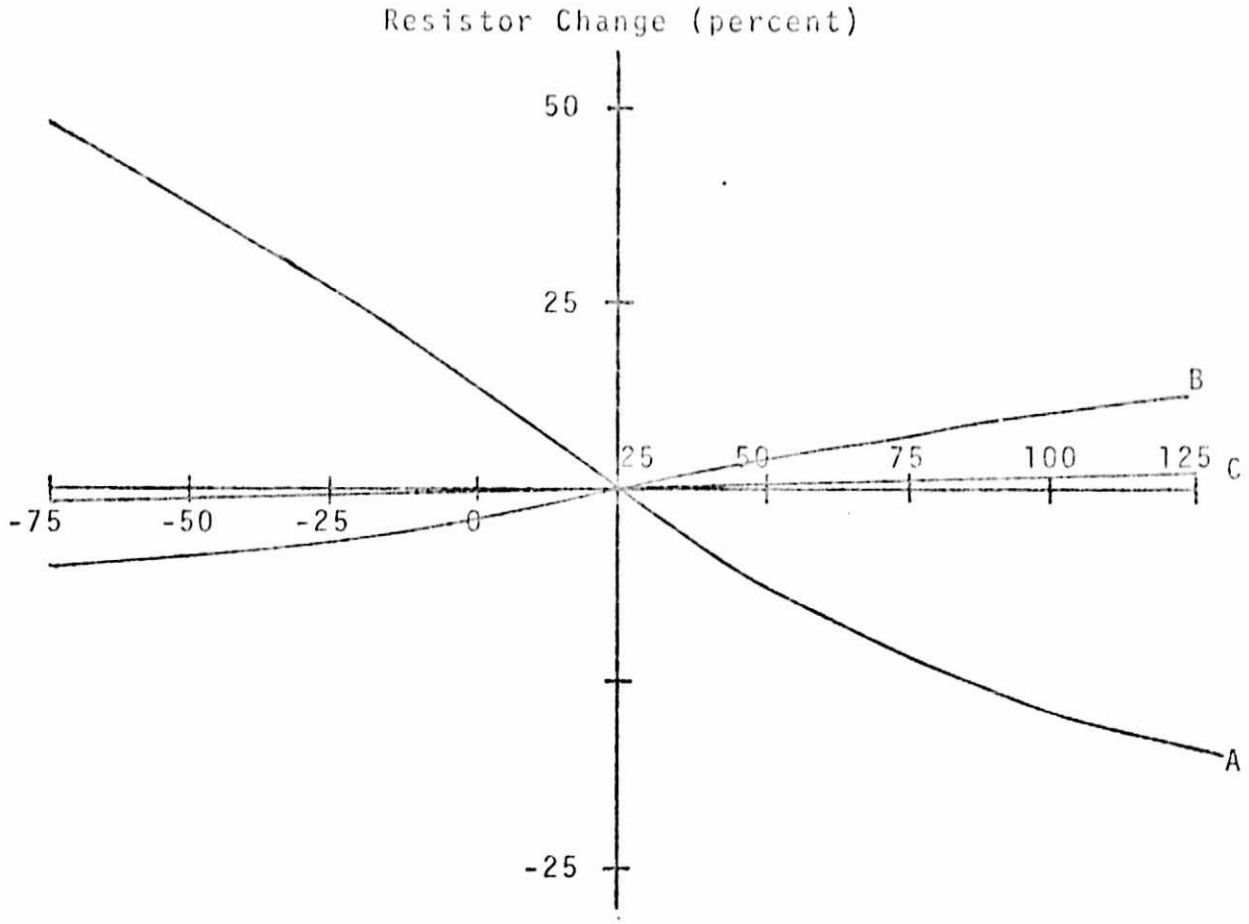

Figure 13. Resistance as a function of temperature for the three pastes examined.

resistance decreased with increasing iron content.

Voltage coefficient of resistance was examined in a power dissipating range from microwatts to 0.3 watts per square cm (2 watts/in^2). Percent change versus power dissipation is plotted in Figure 14. Change in resistance with power loading decreased with increasing iron content.

Conclusions

1. It is feasible to make thick-film resistors from the iron phosphate glass system.

2. Rheology was optimized with an average particle size of 1-3 microns and an upper bound of 7 microns. Organic vehicle of 20 grams ethyl cellulose/liter alpha-terpineol optimized printability with 2.5-3.0 grams of glass frit/milliliter of O.V.

3. The value and stability of iron-phosphate resistors can be controlled by firing procedure and composition.

4. Thick film resistor pastes of the iron-phosphate glass system should be fired near 850°C under a reducing atmosphere such as hydrogen.

5. Conductivity in iron-phosphate resistor systems increases with increasing iron content.

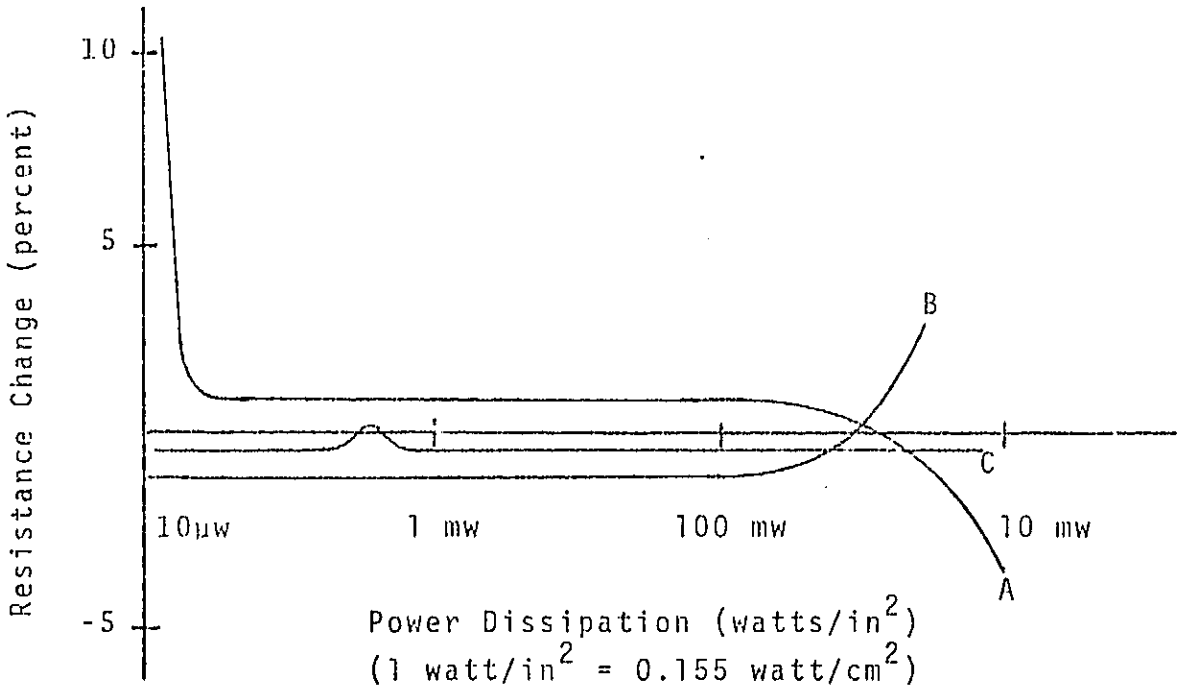

Figure 14. Resistance change as a function of power dissipation.

REFERENCES

1. "Transition Metal Oxide Glass Thick Film Feasibility Study," Dr. J. M. Robertson, School of Engineering Science, (Electrical Engineering) University of Edinburgh, March, 1974.
2. "Correlation Between Structure and Electrical Properties in Iron Phosphate Glasses," J. G. Vaughan, School of Engineering, Vanderbilt University, May, 1974.
3. "The Electrical Resistivity Surface for FeO-Fe_2O_3-P_2O_5 Glasses," J. G. Vaughan and D. L. Kinser, School of Engineering, Vanderbilt University, to be published in Journal of American Ceramic Society, July-August, 1975.
4. "Correlation of Structure and Electrical Properties of $55FeO$-$45P_2O_3$ Glass," A. W. Dozier, L. K. Wilson, E. J. Friebele and D. L. Kinser, Journal of the American Ceramic Society, July, 1972.